HHS Public Access

Author manuscript

Autism Res. Author manuscript; available in PMC 2021 June 11.

Published in final edited form as:

Autism Res. 2021 June ; 14(6): 1101–1114. doi:10.1002/aur.2497.

Children with autism spectrum disorder show altered functional connectivity and abnormal maturation trajectories in response to inverted faces

Fahimeh Mamashli[#1,2], **Nataliia Kozhemiako**[#3,4], **Sheraz Khan**[1,2], **Adonay S. Nunes**[3,4], **Nicole M. McGuiggan**[1], **Ainsley Losh**[1,3], **Robert M. Joseph**[5], **Jyrki Ahveninen**[1,2], **Sam M. Doesburg**[4,6], **Matti S. Hämäläinen**[1,2], **Tal Kenet**[1,3]

[1]Athinoula A. Martinos Center for Biomedical Imaging, MGH/HST, Charlestown, Massachusetts

[2]Department of Radiology, MGH, Harvard Medical School, Boston, Massachusetts

[3]Department of Neurology, MGH, Harvard Medical School, Boston, Massachusetts

[4]Department of Biomedical Physiology and Kinesiology, Simon Fraser University, Vancouver, British Columbia, Canada

[5]Department of Anatomy and Neurobiology, Boston University, Boston, Massachusetts

[6]Behavioral and Cognitive Neuroscience Institute, Simon Fraser University, Vancouver, British Columbia, Canada

[#] These authors contributed equally to this work.

Abstract

The processing of information conveyed by faces is a critical component of social communication. While the neurophysiology of processing upright faces has been studied extensively in autism spectrum disorder (ASD), less is known about the neurophysiological abnormalities associated with processing inverted faces in ASD. We used magnetoencephalography (MEG) to study both long-range and local functional connectivity, with the latter assessed using local cross-frequency coupling, in response to inverted faces stimuli, in 7–18 years old individuals with ASD and age and IQ matched typically developing (TD) individuals. We found abnormally reduced coupling between the phase of the alpha rhythm and the amplitude of the gamma rhythm in the fusiform face area (FFA) in response to inverted faces, as well as reduced long-range functional connectivity between the FFA and the inferior frontal gyrus (IFG) in response to inverted faces in the ASD group. These group differences were absent in response to upright faces. The magnitude of functional connectivity between the FFA and the IFG was significantly correlated with the severity of ASD, and FFA-IFG long-range functional connectivity increased with age in TD group, but not in the ASD group. Our findings suggest that both local and long-range functional connectivity are abnormally reduced in children with ASD when processing inverted faces, and that the pattern of abnormalities associated with the processing of inverted faces differs from the

Correspondence: Tal Kenet, 149, 13th Street, Charlestown, MA, 02129. tal@nmr.mgh.harvard.edu.

CONFLICT OF INTEREST

The authors declare no conflict of interest.

pattern of upright faces in ASD, likely due to the presumed greater reliance on top-down regulations necessary for efficient processing of inverted faces.

Lay Summary:

We found alterations in the neurophysiological responses to inverted faces in children with ASD, that were not reflected in the evoked responses, and were not observed in the responses to upright faces. These alterations included reduced local functional connectivity in the fusiform face area (FFA), and decreased long-range alpha-band modulated functional connectivity between the FFA and the left IFG. The magnitude of long-range functional connectivity between the FFA and the inferior frontal gyrus was correlated with the severity of ASD.

Keywords

autism spectrum disorder; functional connectivity; inverted faces; phase-amplitude coupling

INTRODUCTION

Autism spectrum disorder (ASD) is a neurodevelopmental disorder characterized by impairments in communication, social interactions and repetitive behaviors and restricted interests (American Psychiatric Association, 2013). The processing of information conveyed by faces is a critical component of social communication, and the outstanding ability to process facial information by the human brain is supported by a specialized face processing system that includes the right fusiform face area (FFA; Haxby & Gobbini, 2011; Kanwisher & Yovel, 2006). Given its importance to social communication, many groups have investigated face processing in ASD. While results are somewhat mixed, overall, at least at the neural level, many face-processing related abnormalities have been documented in ASD (Campatelli, Federico, Apicella, Sicca, & Muratori, 2013; Harms, Martin, & Wallace, 2010; Jemel, Mottron, & Dawson, 2006; Weigelt, Koldewyn, & Kanwisher, 2012; Wright et al., 2012). To date, the vast majority of neuroimaging research on face-processing abnormalities in ASD has focused on the processing of upright faces, and relatively few groups have looked at processing of inverted faces in ASD.

The neurophysiological responses to inverted faces are of interest at least in part due to their relevance to the face-inversion effect (FIE). The FIE refers to the observation that while inversion disrupts the recognition of all objects, face inversion produces a greater impairment in face recognition than the impairment produced by the inversion of other images (Bruyer, 2011; Yin, 1969). Early behavioral findings on the FIE in ASD indicated a reduced FIE (Gauthier, Klaiman, & Schultz, 2009; Teunisse & De Gelder, 2003), but more recent studies found no evidence of consistent differences in FIE between ASD and typically developing (TD) individuals but more recent studies found no evidence of consistent differences in FIE between ASD and typically developing (TD) individuals (Tang et al., 2015; Tavares, Mouga, Oliveira, & Castelo-Branco, 2016; Weigelt et al., 2012). Given the somewhat inconsistent findings, the FIE has not garnered significant attention in studies of ASD. Perhaps due to that, the neurophysiology associated with the processing of inverted faces in ASD has been investigated only using a fairly narrow set of neuroimaging measures,

and thus little is known about abnormalities associated with the processing of inverted faces in ASD. Previous studies on the neurophysiology of responses to inverted faces in ASD have reported no differences in averaged cortical evoked responses for upright versus inverted faces (Grice et al., 2001; Khadem, Hossein-Zadeh, & Khorrami, 2016). That said, we have previously shown the more intricate aspects of the neurophysiology underlying ASD can be abnormal even in the presence of seemingly normal evoked responses; more specifically, we have shown that local functional connectivity is abnormal in ASD, even when evoked responses in the FFA elicited by upright faces showed no group differences (Khan et al., 2013; Mamashli et al., 2018), and when evoked responses in the somatosensory cortex elicited by a vibrotactile stimulus applied to the fingertip showed no group differences (e.g., Khan et al., 2015). Whether similar neurophysiological abnormalities manifest in ASD also during the processing of inverted faces has not been investigated.

Gaining a deeper understanding into the neurophysiology of responses to inverted faces ASD is particularly interesting given the evidence that the neurophysiological mechanisms underlying the processing of inverted faces are related to top-down regulation of face perception (Papathomas & Bono, 2004). There is substantial evidence of abnormalities in top-down processing in ASD generally (Cook, Barbalat, & Blakemore, 2012; Frith, 2004; Gomot & Wicker, 2012; Khan et al., 2015; Mamashli et al., 2017; Neumann, Spezio, Piven, & Adolphs, 2006; Seymour, Rippon, Gooding-Williams, Schoffelen, & Kessler, 2019; Sinha et al., 2014), and during face processing particularly (Leung, Ye, Wong, Taylor, & Doesburg, 2014; Loth, Gómez, & Happé, 2010). Thus, investigation of the neurophysiology underlying inverted face processing in ASD could also shed light on top-down regulation abnormalities in ASD more generally.

Here, we used magnetoencephalography (MEG) to explore neurophysiological measures not previously used when analyzing neurophysiological responses to inverted face in ASD. In our prior studies on the processing of upright faces in children and adolescents with ASD, we found that local functional connectivity in the FFA and long range functional connectivity between the FFA and cortical areas involved in top-down regulation were all abnormally reduced in adolescents and young adults with ASD (Khan et al., 2013), but not in children with ASD (Mamashli et al., 2018). Accounting for this discrepancy, we found differences in the maturation trajectories of these local and long-range functional connectivity measures in the ASD group relative to the TD group (Mamashli et al., 2018). At the same time, the evoked responses elicited by the same stimuli, measured as the averaged amplitude of the response over the FFA relative to stimulus onset, and in particular spanning the M170 component of the evoked response, were similar between the TD and ASD groups, irrespective of age. Given these prior findings, we hypothesized that we would again find no group differences in the amplitudes of the evoked responses elicited by inverted faces stimuli within the FFA. In parallel, given that we previously found unaltered local functional connectivity in response to upright faces, measured using phase-amplitude coupling, within the FFA in the same ASD cohort as the current study (Mamashli et al., 2018), and given that there is no evidence of the role of phase-amplitude coupling for processing inverted faces, we hypothesized we will again find this measure unaltered in ASD. Lastly, there is evidence of abnormal top down processing of inverted faces in children with ASD (Bookheimer, Wang, Scott, Sigman, & Dapretto, 2008) and abnormal top-down

processing in ASD in response to faces more generally (Leung et al., 2014; Loth et al., 2010). In parallel, there is evidence of greater reliance on top down processing for inverted faces generally (Fan, Wang, Shao, Zhang, & He, 2020; O'Neil, Hutchison, McLean, & Köhler, 2014; Papathomas & Bono, 2004), alongside evidence of abnormal top-down processing in ASD more generally (Cook et al., 2012; Frith, 2004; Gomot & Wicker, 2012; Khan et al., 2015; Mamashli et al., 2017; Neumann et al., 2006; Seymour et al., 2019; Sinha et al., 2014). Based on these studies, we hypothesized that due to increased or differential recruitment of top-down modulation for processing inverted faces relative to upright faces, we would observe reduced top-down regulation of the FFA, expressed as decreased functional connectivity between frontal areas and the FFA in ASD.

Lastly, we hypothesized that, as in our prior study, we would once again observe a less pronounced maturational trajectory for processing inverted faces in ASD. We studied these measures in the same participants as in our prior study (Mamashli et al., 2018), which allowed us to directly compare cortical responses to upright neutral faces with cortical responses to inverted neutral faces.

METHODS

Participants

Participants were 21 children with ASD, and 27 typically developing (TD) children, aged 7–18 years. The ASD and TD groups were matched for age, and verbal and nonverbal IQ, as measured with the Kaufman Brief Intelligence test (Kaufman & Kaufman, 2004), summarized in Table 1. All Participants were right-handed and had normal or corrected-to-normal vision. All ASD participants had received a clinical diagnosis of ASD prior to the study. In addition, parents completed the Social Communication Questionnaire, Lifetime version (Constantino & Gruber, 2005; Rutter, Bailey, & Lord, 2003) and were administered the Autism Diagnostic Observation Schedule (ADOS-2; Gotham, Risi, Pickles, & Lord, 2007; Hus & Lord, 2014; Lord, Rutter, DiLavore, & Risi, 2008) by trained research personnel to confirm the diagnosis. Final determination of diagnosis for all borderline cases was confirmed by Dr. Joseph, a licensed clinician and ADOS certified trainer. Participants with related medical conditions (e.g., Fragile-X syndrome, tuberous sclerosis) were not included in the study. Parent reports were used to further rule out neurological conditions such as epilepsy, major psychiatric episodes, and substance use over the 6 months prior to enrollment.

Ethical considerations

This study was approved by MGH institutional review board and informed written consent was obtained for every participant and their parents or guardians.

Experimental paradigm

During MEG data collection, participants were presented with pictures of upright neutral, angry, or fearful adult faces (both male and female), pictures of inverted neutral faces, and pictures of houses, in a randomized order. The fearful and angry faces conditions are not included in the present analyses, which focus exclusively on the neutral upright and inverted

faces conditions, and the houses condition. We focused only on the neutral upright faces for this study, because the inverted faces stimuli were also neutral – the same as the upright faces, only inverted. Moreover, the alterations in neural processing of emotional faces in the same cohort was extensively investigated in our previous study (Mamashli et al., 2018). Thus, in this study we analyzed only three stimulus categories from the paradigm described above: houses (at least 150 trial), upright neutral faces (at least 150 trial) and inverted neutral faces (at least 150 trial), as shown schematically in Figure 1. The number of trials per participant per condition ranged from 47 to 156, with no significant differences in the total number of trials per subject between groups, as confirmed by a two-tail *t*-test ($p = 0.18$). Note that only four participants in the ASD group and two in the TD group had fewer than 100 trials per condition.

Each stimulus was displayed on the screen for 1 s followed by intertrial period (fixation cross) for 1 s. The participants were asked to press a button if the same face appeared successively on the screen to ensure attention to the stimuli. Repeat trials were excluded from the analyses. All participants performed at ceiling level on the task. The experiment was broken into 3 runs, each consisting of 50 trials of each stimulus category, where each run lasted about 8 min. The face stimuli were obtained from three datasets: Karolinska Directed Emotional Faces (KDEF; Lundqvist, Flykt, & Ohman, 1998), NimStim Face Stimulus Set (Tottenham et al., 2009), and Gur (Gur et al., 2002). The house stimuli were shared by the Kanwisher Laboratory database at the Massachusetts Institute of Technology. An oval black mask was used to equalize brightness and contrast of the images. The paradigm was written and presented using psychophysics toolbox (Brainard, 1997; Pelli, 1997). Stimuli were presented with a projector onto a back-projection screen placed 100 cm in front of the participant. Participants were given a MEG compatible response pad and instructed to click the response button with their index finger whenever they see the same stimulus repeating (~10% of trials).

Data acquisition

MEG data were collected using a whole-head VectorView MEG system (MEGIN Oy, Finland) inside a magnetically shielded room (IMEDCO). The data were band-passed filtered between 0.1 and 200 Hz and sampled at 600 Hz. Four head position indicator coils (Uutela, Taulu, & Hämäläinen, 2001) were used to record continuous head position and orientation inside the MEG dewar. Prior to the MEG data collection, head shape of the participant, the locations of three fiduciary points (nasion and left and right auricular points), and the four head position indicator coils were digitized using a Fastrak digitizer (Polhemus). This procedure ensured the possibility of the MEG and MRI data co-registration. EOG and ECG electrodes were used to collect signals of ocular and cardiac origin. Real-time averaging of trials without artifacts were used to monitor data quality during acquisition. Additionally, 5 min of empty room data were collected immediately before or immediately after each experimental session, for noise estimation purposes.

Structural MRIs were collected using a 32-channel head coil on a 3.0 T Siemens Trio whole-body MRI scanner (Siemens Medical Systems, Erlangen, Germany) with T1-weighted, high-resolution, magnetization-prepared rapid acquisition gradient-echo (MPRAGE). These data

were processed with Freesurfer to yield cortical reconstruction and parcellations of participants (Dale, Fischl, & Sereno, 1999; Fischl, Sereno, & Dale, 1999). The cortical surface of each hemisphere (~130,000 vertices) was inflated to expose the sulci for better visualization (Dale et al., 1999).

MEG data preprocessing

To supress noise produced by external sources, as well as to correct for head motion within and between runs, MEG data were spatially filtered using signal space separation method (S. Taulu & Simola, 2006; Samu Taulu, Kajola, & Simola, 2004). Note that there was also no significant difference in head motion between the two groups. Signal space projection was employed to remove ocular and cardiac artifacts (Gramfort et al., 2014). Subsequently, the data were bandpassed at 0.1–140 Hz. The data were then split into 1600 ms epochs (400 ms before and 1200 ms after stimulus onset). Epochs with peak-to-peak amplitude above 1000 fT/cm in any of the gradiometers and above 3000 fT in any of magnetometer sensors were excluded from further analysis.

MEG source estimation

We reconstructed the geometry of the cortical surface for each participant based on their T1-weighted MRIs using Freesurfer (Fischl, Sereno, & Dale, 1999). In source estimation, 10,242 approximately equally spaced locations on each cortical hemisphere were used as candidate locations of the cortical dipole sources. A single-compartment boundary-element model (BEM) was used to construct the MEG gain matrix (Hamalainen & Sarvas, 1987; Uutela et al., 2001). The inner skull surface triangulations were generated based on each participant's structural MR images using the watershed algorithm. Minimum-norm estimate (MNE) software was used to estimate the cortical current distributions (http://www.martinos.org/mne). The orientation of the dipoles was fixed to be perpendicular to the cortical surface. Empty room data were used to compute the noise covariance matrix necessary for inverse operator calculation. In order to minimize the bias of the MNEs towards superficial currents, depth weighting was applied (Lin, Belliveau, Dale, & Hämäläinen, 2006). Subsequently, each participant's inflated cortical surface was registered to an average cortical representation (FsAverage in Freesurfer).

Delineation of the FFA and evoked responses

The FFA is defined as the area within the right fusiform gyrus where evoked responses to faces are significantly larger than evoked responses to other stimuli. We used the individual Freesurfer anatomical parcellation to identify the right hemisphere fusiform gyrus in each participant. To then investigate evoked responses, the data were filtered from 0.5 to 40 Hz and epoched from 200 ms before and 500 ms after the stimulus onset. Evoked responses were computed as the total amplitude of this filtered response, irrespective of frequency, at each time point in that window, relative to stimulus onset. Vertex-by-vertex statistical analysis of the evoked response to emotional faces versus the response to evoked houses was used to delineate the FFA. We used a paired t-test (df = 49) to compare the evoked responses to emotional faces with the evoked responses to houses across epochs in each participant. Subsequent t-values were projected to the cortical surface and FFA boundaries were manually delineated based on spatial location of highest t-values. Three Partial Least

Squares (PLS) analyses (Krishnan, Williams, McIntosh, & Abdi, 2011; McIntosh & Lobaugh, 2004) were run to test for group differences in evoked responses in the FFA to inverted faces, to houses, and the difference between responses to inverted versus upright faces. For all evoked responses comparisons between groups or between conditions, 100–250 ms was used as time window of interest. For both conditions (inverted faces and houses) spectral power was estimated for the time period from 0 to 500 ms for alpha and gamma frequency bands (7–13 Hz and 35–120 Hz, respectively), similarly to our prior study on this cohort (Mamashli et al., 2018). The normalized power for each frequency band was computed as subtraction of power during viewing houses, from power during viewing inverted faces and compared between groups using two separate PLS analyses.

Phase amplitude coupling computation in the FFA

Artifact cleaned data filtered from 0.1 to 144 Hz were used to compute PAC. After applying the inverse operator, the data were mapped to the FFA for each participant resulting in 2D matrix (vertices × time). We used the Modulation index (MI) approach, a statistical score that estimates the coupling between two time series, to quantify PAC between alpha (7–13 Hz) phase and gamma (35–120 Hz) amplitude for each voxel as in Mamashli et al., (2018). For each vertex in FFA, the phase was calculated separately for frequency bins from 7 to 13 Hz with 1 Hz steps, and amplitude was estimated for frequencies from 35 to 120 Hz, in 10 Hz steps. Hilbert transformation was used to extract instantaneous phase and amplitude of the signal. To avoid artifacts caused by edge effects, filtering and Hilbert transformation were carried out on continuous data, which then was epoched. Each epoch length was equal to 1000 ms starting with stimulus onset. To eliminate spurious PAC due to sharp edges in the data, all epochs were concatenated into one vector per voxel (Mamashli et al., 2018). We estimated PAC for both inverted faces and houses (PAC was the other conditions was estimated as part of our prior studies). The normalized PAC was then calculated by subtracting PAC during viewing of houses, from PAC during viewing of inverted faces.

Z-coherence between the FFA and IFG, ACC, and precuneus

The three ROIs that showed abnormal coherence in alpha band (8–12 Hz) with the FFA in the ASD group in our prior studies, the IFG, ACC, and precuneus in left hemisphere, were selected in this study, in accordance with the ROIs identified in our prior studies (Khan et al., 2013; Mamashli et al., 2018). We also considered their smaller sub-ROIs (nine sub-ROIs of IFG, four sub-ROIs of ACC, 11 sub-ROIs of precuneus), for the purposes of computing coherence, to increase the signal-to-noise ratio (Mamashli, Khan, Obleser, Friederici, & Maess, 2019). The sub-ROIs were delineated from Freesurfer parcellation using an automatic routine (mris_divide_parcellation) available in the Freesurfer package (equal size principle) to break each large ROI into smaller equal size sub-ROIs; that is, all sub-ROIs in all ROIs were of approximately the same size—thereby increasing the spatial specificity for further connectivity analysis. The location of sub-ROIs for each ROIs is shown on Figure 3a. Signals from each sub-ROI and from the FFA underwent a time-frequency decomposition using complex Morlet wavelets. We computed coherence between FFA and the sub-ROIs of IFG, ACC and precuneus for inverted faces (principal condition) and houses (baseline condition). Subsequently, *Z*-Coherence were calculated by normalizing the principal condition coherence values by the baseline condition for the purpose of eliminating a

statistical bias caused by the non-Gaussian distribution of coherence values and unequal sample sizes (Maris & Oostenveld, 2007).

Statistical analysis of between group differences

To test for group differences in evoked responses, normalized PAC, and *Z*-coherence, we used mean-centered Partial Least Squares (PLS) analysis (Krishnan et al., 2011; McIntosh & Lobaugh, 2004). PLS is a multivariate nonparametric statistical approach for testing the significance of differences between groups or conditions. Mathematically it is based on singular value decomposition of the data in order to extract latent variables which account for the variance in the data (Lobaugh, West, & McIntosh, 2001). Subsequent global test based on random permutations of subjects between groups results in one *p* value for each latent variable that indicates the significance of group differences. Note that by using this permutations based approach, we generated a null distribution of *p* values based on the data, thus eliminating the need to assume the data follow a normal distribution. Each latent variable captures all data features at once, thus avoiding the need for separate tests for each data feature, and thereby addressing the multiple comparison problems. To investigate the contribution of each data feature to group differences the series of bootstrapping is performed. As a result, each data feature is assigned with a bootstrap ratio value that also can be referred to as a PLS *z*-score. The data features (e.g., frequency bins in case of PAC comparison or timepoints in case of ERF comparison) with the highest absolute PLS *z*-score are the ones where the group differences are the most robust. In this article, we use the PLS *z*-score threshold of 3 and −3 as it approximately corresponds to the limits of the 99% confidence interval (Krishnan et al., 2011; McIntosh & Lobaugh, 2004).

Three PLS analyses were used to compare evoked responses between groups for inverted faces and houses conditions, each separately, and the difference between inverted and upright neutral faces in the time window of 100–250 ms following stimulus onset. One PLS analysis was performed to test for group differences in normalized PAC within the FFA, for the frequency range 35–120 Hz. Two PLS analyses were run to compare normalized spectral power of alpha (7–13 Hz) and gamma frequency (35–120 Hz) in the 0–500 ms time window, to ensure that PAC results were not caused by differences in power. Three additional PLS analyses were carried out to compare *Z*-coherence between FFA and sub-ROIs of IFG, ACC and precuneus, for the frequency range of 8–12 Hz averaged across 100–250 ms after stimulus onset. For all of our PLS analysis, we used 5000 permutations and 5000 bootstrapping series.

Association between PAC and Z-coherence

To test for a significant correlation between the magnitude of normalized PAC in right FFA and the magnitude of *Z*-coherence in the alpha band between the right FFA and the left IFG, both in response to inverted faces, we used a one-tailed Pearson correlation. To that end, we normalized PAC in frequencies where group differences were the strongest (PLS *z*-score ≥ 3) and averaged *Z*-coherence in frequencies and sub-ROIs with PLS *z*-score ≥ 3.

Association with age and ASD symptoms severity

To investigate the association between normalized PAC and age and ASD symptom severity, we focused on the frequencies where group differences were the strongest (PLS *z*-score ≥3). Normalized PAC values in the frequencies that exceeded that threshold were averaged, and the one-tailed Pearson's correlation with age (in both the TD and the ASD groups) or symptom severity (in the ASD group) was computed. We used a one-tailed Pearson's correlation because the directions of expected correlations were formulated based on our previous findings (Khan et al., 2013; Mamashli et al., 2018). Symptom severity was measures using the SRS total *t*-score and ADOS social-affective sub-score. Association of *Z*-coherence with age and symptoms severity were tested in similar way.

Classification of ASD versus TD based on normalized PAC and Z-coherence

We used a Support Vector Machine algorithm with a linear kernel (as implemented in Scikit-Learn) to predict diagnosis (Pedregosa et al., 2011). We selected features based on our group differences results: (a) averaged normalized PAC in frequencies where group differences were the strongest (PLS *z*-score ≥ 3); (b) averaged alpha band *Z*-coherence in frequencies and sub-ROIs with PLS *z*-score ≥ 3. The classification accuracy was assessed using a threefold cross-validation.

RESULTS

Evoked responses to inverted faces and houses

We began by assessing whether there were any significant group differences in the evoked responses for inverted faces (Figure 2a), evoked responses for houses (Figure 2b) and the difference in evoked responses for inverted faces versus neutral faces (Figure 2c), in the FFA (Figure 2d), using a Partial Least Squares (PLS) analysis. We found no significant group differences in evoked responses for any of the above comparisons.

Local functional connectivity in the FFA

We assessed local functional connectivity using a specific subset of cross-frequency coupling: Phase-Amplitude Coupling (PAC; Khan et al., 2013; Mamashli et al., 2018). PAC is a measure of the extent to which the amplitude of a faster frequency band (here, gamma, 35–120 Hz) is modulated by the phase of a slower frequency band (alpha, 7–13 Hz). PAC reflects aspects of local functional connectivity because it varies on very short spatial scales in the cortex (~1 cm), as shown using subdural electrocorticogram (Canolty et al., 2006). We found no significant group differences in PAC within condition during viewing of inverted faces, or during viewing of houses. We therefore assessed the normalized PAC, PAC during the inverted faces relative to PAC during the houses condition. The comparison of normalized PAC estimated in FFA in the frequency range of 35–120 Hz revealed significant differences ($p = 0.01$) between the ASD and TD groups. The group contrast showed a positively skewed PLS *z*-score distribution, indicating that the TD group had higher normalized PAC than the ASD group (Figure 3a,b). To identify the frequency bands where group differences were the most pronounced, we used a PLS *z*-score threshold of 3 (Figure 3c). The group differences with the largest difference were in the frequency range of 50–55

Hz. There was a strong trend towards significance also around 80 Hz, but this trend did not meet significance at the chosen threshold. Note that alpha and gamma bands power for the same time period was not significantly different ($p > 0.05$) between the two groups as confirmed by two separate PLS analyses; thus, any group differences in PAC were not due to power differences.

Long-range connectivity between FFA and IFG, ACC and precuneus

In our prior study of face processing in adolescents and young adults with ASD, responses to upright emotional faces, the IFG, ACC and precuneus all showed abnormally reduced long-range connectivity between the FFA and each of three regions of interest (ROIs)—the IFG, ACC, and precuneus. Here, we compared long-range functional connectivity in response to inverted versus upright neutral faces between the FFA and each of these same three ROIs—IFG, ACC and precuneus—using *Z*-coherence, in the alpha frequency band. *Z*-coherence was defined as coherence while viewing inverted faces normalized by coherence while viewing houses. To maximize power when assessing *Z*-coherence, we computed *Z*-coherence for multiple subdivisions of each of the ROIs (Mamashli, Hämäläinen, Ahveninen, Kenet, & Khan, 2019). There were no group differences in *Z*-coherence between the FFA and either the precuneus or the ACC, while *Z*-Coherence between FFA and the IFG was significantly reduced in the ASD group ($p = 0.004$, Figure 4a). Figure 4b illustrates the distribution of *z*-score across all sub-ROIs of the IFG, revealing that group differences were strongest in the inferior sub-ROIs of IFG, with a consistent trend across all sub-ROIs, even the ones that did not reach significance. The group contrast is shown in Figure 4c, and the distribution of PLS *z*-scores is shown in Figure 4d.

Correlation between PAC and Z-coherence

In our prior studies (Khan et al., 2013; Mamashli et al., 2018), we examined whether the magnitude of PAC was correlated with the magnitude of FFA-IFG connectivity. In our 2013 study of adolescents and young adults, we found that PAC and long-range functional connectivity during viewing of emotional upright faces were indeed correlated. In contrast, in our 2018 study of the cohort examined here, we found no such correlation, again during viewing of emotional, as well as neutral, upright faces. Here, we found that once again, there was a significant correlation between the magnitude of PAC and the magnitude of IFG-FFA functional connectivity when the two groups were combined, and there was a trend towards such a correlation within each group (Figure 5).

Correlations of PAC and Z-coherence with age

In our prior study of responses to upright faces in this cohort, we found a divergence in the maturation trajectories of functional connectivity between the groups, and tested for a similar effect here, using both PAC and IFG-FFA functional connectivity. We found no significant correlation between PAC in response to inverted faces, and age. In contrast, *Z*-coherence between the FFA and all IFG subdivisions thresholded at PLS *z*-score ≥ 3 was significantly correlated with age in the TD group ($R = 0.35$, $p = 0.039$), but such a correlation was absent in the ASD group (Figure 6).

Z-coherence and PAC correlations with ASD symptoms severity

To assess whether the neurophysiological measures correlated with the ASD phenotype, we focused on two ASD severity measures that assess the social communication and reciprocal social interaction domains of ASD severity: the SRS (Social Responsiveness Scale), and the social affective sub-score from the ADOS-2 (Autism Diagnostic Observation Schedule) Module 3 and 4 diagnostic algorithms ($ADOS_{SA}$). *Z*-coherence between the FFA and IFG (averaged across IFG subdivisions thresholded at PLS *z*-score ≥ 3) in the ASD group was significantly correlated with both measures of ASD severity: the SRS total *t*-score ($r = -0.38$, $p = 0.046$; Figure 7a), and the $ADOS_{SA}$ score ($r = -0.438$, $p = 0.024$, Figure 7b), indicating that greater ASD severity corresponded to greater reductions in *Z*-coherence. In contrast, PAC was not correlated with either of the ASD symptom severity measures.

Classification by diagnosis based on normalized PAC and Z-coherence

Lastly, we used linear support vector machines (LSVM) to carry out a blind classification by group (ASD vs. TD) using PAC and *Z*-Coherence (FFA to all IFG subdivisions thresholded at PLS *z*-score ≥ 3). Figure 7c shows the model, which had a classification accuracy of 81% ± 4%, relative to the 56% chance level (higher than 50% due to the unequal group sizes).

DISCUSSION

We investigated local and long-range functional connectivity alterations in response to inverted faces, in children with ASD. As expected from our prior studies of upright faces (Khan et al., 2013; Mamashli et al., 2018), and studies of others of inverted faces (Tavares et al., 2016; Webb et al., 2012), we did not find group differences in evoked responses elicited by neutral upright faces, neutral inverted faces, or houses. In contrast, we did find reduced local functional connectivity in the FFA in ASD compared to TD participants, measured using PAC. Furthermore, we found reduced long-range functional connectivity in the alpha frequency band between the FFA and the IFG in the ASD group. These findings were specific to the processing of inverted faces, since our prior investigation in the same cohort of children, that focused exclusively on the processing of upright faces, showed no differences in local or long range functional connectivity measures between the ASD and TD groups (Mamashli et al., 2018). In addition, in our study of the processing of upright faces in ASD in adolescents and young adults, three distinct top-down cortical regions showed reduced long-range functional connectivity with the FFA: The precuneus, the ACC, and the IFG. In this study, reduced long-range functional connectivity was only observed between IFG and the FFA. Importantly, reduced functional connectivity between the IFG and the FFA was correlated with more severe ASD symptomatology. In addition, functional connectivity between the IFG and the FFA increased with age in the TD group, but not the ASD group. Lastly, alterations in both local and long-range functional connectivity predicted the participants' diagnosis with 81% accuracy indicating the potential value of this approach for ASD classification in future cohorts.

We have previously shown that PAC is abnormally reduced in adolescents and young adults with ASD when viewing emotional faces, but that this was not the case for younger children with ASD (Mamashli et al., 2018). Therefore, although abnormally reduced resting-state

PAC had been previously documented in other brain areas in younger participants with ASD (Port, Dipiero, et al., 2019), we did not expect to find reduced PAC in the FFA in response to inverted faces.

One potential hypothesis regarding the neural mechanisms that may underlie the unexpected finding of reduced PAC in ASD during viewing of inverted faces stems from the reliance of PAC on inhibitory processes in the brain. PAC is known to be modulated by GABAergic signaling, and specifically by parvalbumin expressing (PV^+) interneurons (Lopez-Pigozzi et al., 2016; Michaels, Long, Stevenson, Chrobak, & Chen, 2018; Port, Berman, et al., 2019; Wulff et al., 2009). This is relevant because studies of genetics-based mouse models of ASD have consistently found underdeveloped PV^+ interneurons (e.g., Han et al., 2012; Nakai et al., 2014), and abnormalities in densities of PV^+ interneurons have also been documented in postmortem studies of ASD brains (e.g., Hashemi, Ariza, Rogers, Noctor, & Martínez-Cerdeño, 2017). If the processing of inverted faces were to require recruitment of additional inhibitory processing relative to upright faces, this could in turn impact PAC. While there is no direct evidence of additional recruitment of inhibitory processes during viewing of inverted faces, there is some evidence that more generally recruitment of resources for processing inverted faces is abnormal in ASD, as suggested by some ERP studies (McPartland, Dawson, Webb, Panagiotides, & Carver, 2004; Rossion et al., 2000; Webb et al., 2012). If this recruitment includes GABAergic resources, as may well be the case, this could result in the group differences in PAC between ASD and TD groups when viewing inverted faces relative to upright faces, as observed here.

Evidence that the processing of inverted faces relies on top-down regulation of face perception (Papathomas & Bono, 2004) provides another potential explanation for our finding of reduced PAC. The lack of differences in general properties (such as color, shapes, number of features, etc.) between upright and inverted faces suggests that low level mechanisms of perception are not responsible for the face inversion effect. Here, we found reduced long-range communication in the alpha band between the IFG and FFA in ASD. While the finding was not direction specific, the putative role of the IFG in top down modulation (Gazzaley & Nobre, 2012; Mayer et al., 2007) supports a likely explanation for this observation where the top-down modulation of the FFA by the IFG is reduced in individuals with ASD when viewing inverted faces. Indeed, these alterations were associated with severity of ASD. This finding is also consistent with our initial hypothesis of reduced top-down regulation in ASD.

It is also possible that reduced long-range top-down modulation is causative, at least in part, of the observed reduction in local functional connectivity as measured using PAC. Indeed, the correlation we observed between the magnitude of PAC and the magnitude of the IFG-FFA functional connectivity suggests such an interaction. It has been previously hypothesized that communication across different scales in the brain is modulated by coherence, and that the directionality of influence depends on the long-range modulation of local PAC connectivity (Canolty & Knight, 2010; Fries, 2005, 2009, 2015; Krishnan et al., 2011; Lega, Burke, Jacobs, & Kahana, 2016).

The reduction in top-down modulations documented here is also consistent with multiple reports of abnormalities in top-down processing in ASD (Cook et al., 2012; Frith, 2004; Gomot & Wicker, 2012; Khan et al., 2015; Mamashli et al., 2017; Neumann et al., 2006; Seymour et al., 2019; Sinha et al., 2014), including during face processing (Leung et al., 2014; Loth et al., 2010). It has been suggested that ASD-related atypicalities stem mostly from reduced flow of feedback information, resulting in impaired top-down modulation (Frith, 2004). More recently, deficient top-down control was hypothesized to disrupt the predictive ability of the brain and to be causative of hallmark features of ASD, including insistence of sameness, sensory hypersensitivity and theory of mind deficits (Sinha et al., 2014). Lastly, reduced top-down regulation during face processing in particular, was linked to failure to efficiently extract emotional information from faces or reconstruct the degraded pictures of faces (Leung et al., 2014; Loth et al., 2010).

The reduced PAC and *Z*-coherence in children with ASD in response to inverted faces may also relate to findings of reduction or absence of the FIE in ASD relative to TD children. While we have not investigated the FIE directly here, this is relevant because it has been postulated that the FIE is driven by the necessity to switch from holistic face processing to evaluation of face parts separately, since inversion precludes the use of configural information required for holistic processing, such as distance and relative position of face parts, while featural information, such as size and shape of face parts, is preserved (Freire, Lee, & Symons, 2000). This would suggest that in individuals with ASD, the holistic way of face processing is not established to the same degree as in TD individuals, which is supported by other evidence as well (Behrmann, Thomas, & Humphreys, 2006). Accordingly, additional top-down modulation for reconfiguration from holistic face processing to fragmentary face processing would be superfluous.

Lastly, we also found that *Z*-coherence between the FFA and the IFG increased with age in the TD group, but this maturation effect was absent in the ASD group. This is congruent with extensive reports of top-down regulation improvement and increased processing efficiency with age in TD individuals (Casey & Jones, 2010; Rubia, 2013) and altered neurocognitive developmental trajectories in ASD (Dajani & Uddin, 2016; Kitzbichler et al., 2015; Kozhemiako et al., 2020, 2019; Mamashli et al., 2018; Vakorin et al., 2017). There is also evidence that the FIE effect increases with age in typical individuals (de Heering, Rossion, & Maurer, 2012), furthering the line of evidence in support of the processing of upright faces getting more efficient with age, while the processing of inverted faces does not, which might further explain our results of a positive correlation between age and *Z*-coherence in TD group but not in ASD group.

The interpretation of these results with respect to the FIE in ASD are limited since behavioral FIE data were not available for this cohort. Thus, while the neurophysiological results refer to cortical processing of inverted faces, an important limitation of this study is that it cannot be extended to infer about the FIE in ASD more generally, due to lack of behavioral data. In addition, the limited sample size means that further replication of these results is warranted, and that other potential abnormalities associated with this response may not have been detectable with this sample size. The same limitation also applies to the results showing abnormal maturational trajectories in the ASD group, which would benefit

from a higher age density. That said, the findings of reduced local and long-range functional connectivity in the ASD group as well as the finding of abnormal maturation of functional connectivity in the ASD group, are both consistent with other related studies noted above, showing reduced PAC and flattened maturation trajectories in ASD across a range of paradigms. This consistency with prior studies therefore increases the confidence in the validity of the results in spite of the relatively small sample size. Another limitation is that no eye tracking was available during the recording, and participants' attention was only ensured through the one-back task (~10% of trials). While there was no difference in performance on the one-back task between the groups, it is of course not as accurate as eye tracking, nor is it continuous. Lastly, in spite of these limitations, the correlations between the neurophysiological data and behavioral ASD data indicate that the results are likely to remain consistent in larger populations.

In conclusion, the results of the present study show multiple alterations in the processing of inverted faces in the ASD group, but no differences in the evoked responses to inverted faces between the two groups. The abnormalities mapped in the ASD group included reduced local functional connectivity in the FFA, and decreased long-range alpha-band modulated functional connectivity between the FFA and the left IFG. These results align well with hypotheses that reduced top-down regulation in ASD impairs the processing of inverted faces, and with the hypothesis that GABAergic modulations are abnormal in ASD. These results also suggest that the maturational trajectories of face processing in ASD diverge from typical development earlier for inverted faces than for upright faces, perhaps due to a greater reliance on GABAergic mechanisms and top-down modulation when processing inverted faces. In summary, our results suggest that the neurophysiological abnormalities that underlie ASD are often more subtle than effects detectable using common measures such as evoked responses, can vary with specific details of the paradigm, for example, inverted versus upright faces, and are age dependent. These results further underscore the importance of considering age when investigating the neurophysiology that underlies ASD, and the importance of exploring the neurophysiological substrates of ASD using a wide range of methodologies and approaches.

ACKNOWLEDGMENTS

This study was supported by grants from the Nancy Lurie Marks Family Foundation (Tal Kenet, Sheraz Khan), Autism Speaks (Tal Kenet), The Simons Foundation (SFARI 239395, Tal Kenet), The National Institute of Child Health and Development (R01HD073254, Tal Kenet), The National Institute of Mental Health (R01MH117998, R21MH116517, Tal Kenet), National Institute for Biomedical Imaging and Bioengineering (P41EB015896, Matti Hämäläinen), National Institute of Neurological Disorders and Stroke (R01NS104585, Matti Hämäläinen) and National Institute on Deafness and Other Communication Disorders (R01DC016915, R01DC016765, Jyrki Ahveninen), Canadian Institutes of Health Research (MOP-136935, Sam M. Doesburg). Article needs to be deposited in PMC.

DATA AVAILABILITY STATEMENT

The data that support the findings of this study are available from the corresponding author upon reasonable request.

REFERENCES

American Psychiatric Association. (2013). Diagnostic and statistical manual of mental disorders. American Psychiatric Publishing, Inc. 10.1176/appi.books.9780890425596

Behrmann M, Thomas C, & Humphreys K (2006). Seeing it differently: Visual processing in autism. Trends in Cognitive Sciences, 10 (6), 258–264. 10.1016/j.tics.2006.05.001 [PubMed: 16713326]

Bookheimer SY, Wang AT, Scott A, Sigman M, & Dapretto M (2008). Frontal contributions to face processing differences in autism: Evidence from fMRI of inverted face processing. Journal of the International Neuropsychological Society, 14(6), 922–932. 10.1017/S135561770808140X [PubMed: 18954473]

Brainard DH (1997). The psychophysics toolbox. Spatial Vision, 10 (4), 433–436. 10.1163/156856897X00357 [PubMed: 9176952]

Bruyer R (2011). Configural face processing: A meta-analytic survey. Perception, 40(12), 1478–1490. 10.1068/p6928 [PubMed: 22474766]

Campatelli G, Federico RR, Apicella F, Sicca F, & Muratori F (2013). Face processing in children with ASD: Literature review. Research in Autism Spectrum Disorders, 7, 444–454. 10.1016/j.rasd.2012.10.003

Canolty RT, & Knight RT (2010, 11 1). The functional role of cross-frequency coupling. Trends in Cognitive Sciences, 14, 506–515. 10.1016/j.tics.2010.09.001 [PubMed: 20932795]

Canolty RT, Edwards E, Dalal SS, Soltani M, Nagarajan SS, Kirsch HE, Berger MS, Barbaro NM, & Knight RT (2006). High gamma power is phase-locked to theta oscillations in human neocortex. Science, 313(5793), 1626–1628. 10.1126/science.1128115 [PubMed: 16973878]

Casey BJ, & Jones RM (2010). Neurobiology of the adolescent brain and behavior: Implications for substance use disorders. Journal of the American Academy of Child and Adolescent Psychiatry, 49(12), 1189–1201. 10.1016/j.jaac.2010.08.017 [PubMed: 21093769]

Constantino JN, & Gruber CP (2005). The social responsiveness scale (SRS). Los Angeles: Western Psychological Services.

Cook J, Barbalat G, & Blakemore SJ (2012). Top-down modulation of the perception of other people in schizophrenia and autism. Frontiers in Human Neuroscience, 6(175), 1–10. 10.3389/fnhum.2012.00175 [PubMed: 22279433]

Dajani DR, & Uddin LQ (2016). Local brain connectivity across development in autism spectrum disorder: A cross-sectional investigation. Autism Research, 9(1), 43–54. 10.1002/aur.1494 [PubMed: 26058882]

Dale AM, Fischl B, & Sereno MI (1999). Cortical surface-based analysis: I. Segmentation and surface reconstruction. NeuroImage, 9(2), 179–194. 10.1006/nimg.1998.0395 [PubMed: 9931268]

de Heering A, Rossion B, & Maurer D (2012). Developmental changes in face recognition during childhood: Evidence from upright and inverted faces. Cognitive Development, 27(1), 17–27. 10.1016/j.cogdev.2011.07.001

Fan X, Wang F, Shao H, Zhang P, & He S (2020). The bottom-up and top-down processing of faces in the human occipitotemporal cortex. eLife, 9. 10.7554/eLife.48764

Fischl B, Sereno MI, & Dale AM (1999). Cortical surface-based analysis: II. Inflation, flattening, and a surface-based coordinate system. NeuroImage, 9(2), 195–207. 10.1006/nimg.1998.0396 [PubMed: 9931269]

Freire A, Lee K, & Symons LA (2000). The face-inversion effect as a deficit in the encoding of configural information: Direct evidence. Perception, 29(2), 159–170. 10.1068/p3012 [PubMed: 10820599]

Fries P (2005). A mechanism for cognitive dynamics: Neuronal communication through neuronal coherence. Trends in Cognitive Sciences, 9(10), 474–480. 10.1016/j.tics.2005.08.011 [PubMed: 16150631]

Fries P (2009). Neuronal gamma-band synchronization as a fundamental process in cortical computation. Annual Review of Neuroscience, 32(1), 209–224. 10.1146/annurev.neuro.051508.135603

Fries P (2015). Rhythms for cognition: communication through coherence. Neuron, 88(1), 220–235. 10.1016/j.neuron.2015.09.034 [PubMed: 26447583]

Frith C (2004, 10 1). Is autism a disconnection disorder? Lancet Neurology, 3, 577. 10.1016/S1474-4422(04)00875-0 [PubMed: 15380151]

Gauthier I, Klaiman C, & Schultz RT (2009). Face composite effects reveal abnormal face processing in autism spectrum disorders. Vision Research, 49(4), 470–478. 10.1016/j.visres.2008.12.007 [PubMed: 19135077]

Gazzaley A, & Nobre AC (2012). Top-down modulation: Bridging selective attention and working memory. Trends in Cognitive Sciences, 16, 129–135. 10.1016/j.tics.2011.11.014 [PubMed: 22209601]

Gomot M, & Wicker B (2012). A challenging, unpredictable world for people with autism spectrum disorder. International Journal of Psychophysiology, 83, 240–247. 10.1016/j.ijpsycho.2011.09.017 [PubMed: 21968196]

Gotham K, Risi S, Pickles A, & Lord C (2007). The autism diagnostic observation schedule: Revised algorithms for improved diagnostic validity. Journal of Autism and Developmental Disorders, 37(4), 613–627. 10.1007/s10803-006-0280-1 [PubMed: 17180459]

Gramfort A, Luessi M, Larson E, Engemann DA, Strohmeier D, Brodbeck C, Parkkonen L, & Hämäläinen MS (2014). MNE software for processing MEG and EEG data. NeuroImage, 86, 446–460. 10.1016/j.neuroimage.2013.10.027 [PubMed: 24161808]

Grice SJ, Spratling MW, Karmiloff-Smith A, Halit H, Csibra G, de Haan M, & Johnson MH (2001). Disordered visual processing and oscillatory brain activity in autism and Williams syndrome. Neuroreport, 12(12), 2697–2700.Retrieved from. https://journals.lww.com/neuroreport/Abstract/2001/08280Disordered_visual_processing_and_oscillatory_brain.21.aspx [PubMed: 11522950]

Gur RC, Sara R, Hagendoorn M, Marom O, Hughett P, Macy L, Turner T, Bajcsy R, Posner A, & Gur RE (2002). A method for obtaining 3-dimensional facial expressions and its standardization for use in neurocognitive studies. Journal of Neuroscience Methods, 115(2), 137–143. 10.1016/S0165-0270(02)00006-7 [PubMed: 11992665]

Hamalainen MS, & Sarvas J (1987). Feasibility of the homogeneous head model in the interpretation of neuromagnetic fields. Physics in Medicine and Biology, 32(1), 91–97. 10.1088/0031-9155/32/1/014 [PubMed: 3823145]

Han S, Tai C, Westenbroek RE, Yu FH, Cheah CS, Potter GB, Rubenstein JL, Scheuer T, de la Iglesia HO, & Catterall WA (2012). Autistic-like behaviour in Scn1a ± mice and rescue by enhanced GABA-mediated neurotransmission. Nature, 489(7416), 385–390. 10.1038/nature11356 [PubMed: 22914087]

Harms MB, Martin A, & Wallace GL (2010, 9 1). Facial emotion recognition in autism spectrum disorders: A review of behavioral and neuroimaging studies. Neuropsychology Review, 20, 290–322. 10.1007/s11065-010-9138-6 [PubMed: 20809200]

Hashemi E, Ariza J, Rogers H, Noctor SC, & Martínez-Cerdeño V (2017). The number of parvalbumin-expressing interneurons is decreased in the prefrontal cortex in autism. Cerebral Cortex, 27(3), 1931–1943. 10.1093/cercor/bhw021 [PubMed: 26922658]

Haxby JV, & Gobbini IM (2011). Distributed neural systems for face perception. In Calder A, Rhodes G, Johnson M, & Haxby J (Eds.), Oxford handbook of face perception (pp. 93–110). Oxford: Oxford University Press. Retrieved from https://books.google.ca/books?hl=en&lr=&id=2UXx9rdfriQC&oi=fnd&pg=PA93&dq=gobbini+haxby+2006&ots=ZEhvoT4OjC&sig=6DZozO2aCZoECCW9-4zY4KV-EfE#v=onepage&q=gobbinihaxby2006&f=false

Hus V, & Lord C (2014). The autism diagnostic observation schedule, module 4: Revised algorithm and standardized severity scores. Journal of Autism and Developmental Disorders, 44(8), 1996–2012. 10.1007/s10803-014-2080-3 [PubMed: 24590409]

Jemel B, Mottron L, & Dawson M (2006, 1 14). Impaired face processing in autism: Fact or artifact? Journal of Autism and Developmental Disorders, 36, 91–106. 10.1007/s10803-005-0050-5 [PubMed: 16477517]

Kanwisher N, & Yovel G (2006). The fusiform face area: A cortical region specialized for the perception of faces. *Philosophical Transactions of the Royal Society B*: Biological Sciences, 361(1476), 2109–2128. 10.1098/rstb.2006.1934 [PubMed: 17118927]

Kaufman AS, & Kaufman NL (2004). Kaufman brief intelligence test (2nd ed.). San Antonio, TX: Pearson Assessments. 10.1002/9781118660584.ese1325

Khadem A, Hossein-Zadeh GA, & Khorrami A (2016). Long-range reduced predictive information transfers of autistic youths in EEG sensor-space during face processing. Brain Topography, 29 (2), 283–295. 10.1007/s10548-015-0452-4 [PubMed: 26433373]

Khan S, Gramfort A, Shetty NR, Kitzbichler MG, Ganesan S, Moran JM, Lee SM, Gabrieli JD, Tager-Flusberg HB, Joseph RM, Herbert MR, Hämäläinen MS, & Kenet T (2013). Local and long-range functional connectivity is reduced in concert in autism spectrum disorders. Proceedings of the National Academy of Sciences of the United States of America, 110(8), 3107–3112. 10.1073/pnas.1214533110 [PubMed: 23319621]

Khan S, Michmizos K, Tommerdahl M, Ganesan S, Kitzbichler MG, Zetino M, Garel KLA, Herbert MR, Hämäläinen MS, & Kenet T (2015). Somatosensory cortex functional connectivity abnormalities in autism show opposite trends, depending on direction and spatial scale. Brain, 138(5), 1394–1409. 10.1093/brain/awv043 [PubMed: 25765326]

Kitzbichler MG, Khan S, Ganesan S, Vangel MG, Herbert MR, Hämäläinen MS, & Kenet T (2015). Altered development and multifaceted band-specific abnormalities of resting state networks in autism. Biological Psychiatry, 77(9), 794–804. 10.1016/j.biopsych.2014.05.012 [PubMed: 25064418]

Kozhemiako N, Vakorin V, Nunes AS, Iarocci G, Ribary U, & Doesburg SM (2019). Extreme male developmental trajectories of homotopic brain connectivity in autism. Human Brain Mapping, 40(3), 987–1000. 10.1002/hbm.24427 [PubMed: 30311349]

Kozhemiako N, Nunes AS, Vakorin V, Iarocci G, Ribary U, & Doesburg SM (2020). Alterations in local connectivity and their developmental trajectories in autism spectrum disorder: Does being female matter? Cerebral Cortex, 30, 1–14. 10.1093/cercor/bhaa109 [PubMed: 31220218]

Krishnan A, Williams LJ, McIntosh AR, & Abdi H (2011). Partial least squares (PLS) methods for neuroimaging: A tutorial and review. NeuroImage, 56(2), 455–475. 10.1016/j.neuroimage.2010.07.034 [PubMed: 20656037]

Lega B, Burke J, Jacobs J, & Kahana MJ (2016). Slow-theta-to-gamma phase-amplitude coupling in human hippocampus supports the formation of new episodic memories. Cerebral Cortex, 26 (1), 268–278. 10.1093/cercor/bhu232 [PubMed: 25316340]

Leung RC, Ye AX, Wong SM, Taylor MJ, & Doesburg SM (2014). Reduced beta connectivity during emotional face processing in adolescents with autism. Molecular Autism, 5(1), 51. 10.1186/2040-2392-5-51 [PubMed: 25371811]

Lin F-H, Belliveau JW, Dale AM, & Hämäläinen MS (2006). Distributed current estimates using cortical orientation constraints. Human Brain Mapping, 27(1), 1–13. 10.1002/hbm.20155 [PubMed: 16082624]

Lobaugh NJ, West R, & McIntosh AR (2001). Spatiotemporal analysis of experimental differences in event-related potential data with partial least squares. Psychophysiology, 38(3), 517–530. Retrieved from http://www.ncbi.nlm.nih.gov/pubmed/11352141 [PubMed: 11352141]

Lopez-Pigozzi D, Laurent F, Brotons-Mas JR, Valderrama M, Valero M, Fernandez-Lamo I, Cid E, Gomez-Dominguez D, Gal B, & Menendez de la Prida L (2016). Altered oscillatory dynamics of CA1 parvalbumin basket cells during theta-gamma rhythmopathies of temporal lobe epilepsy. ENeuro, 3(6), 1–20. 10.1523/ENEURO.0284-16.2016

Lord C, Rutter M, DiLavore P, & Risi S (2008). ADOS: Autism diagnostic observation schedule. Boston, MA: Hogrefe.

Loth E, Gómez JC, & Happé F (2010). When seeing depends on knowing: Adults with autism Spectrum conditions show diminished top-down processes in the visual perception of degraded faces but not degraded objects. Neuropsychologia, 48(5), 1227–1236. 10.1016/j.neuropsychologia.2009.12.023 [PubMed: 20026140]

Lundqvist D, Flykt A, & Ohman A (1998). The Karolinska directed emotional faces (KDEF). CD ROM Stockholm: Department of Clinical Neuroscience, Psychology Section, Karolinska Institutet.

Mamashli F, Khan S, Bharadwaj H, Michmizos K, Ganesan S, Garel K-LA, Ali Hashmi J, Herbert MR, Hämäläinen M, & Kenet T (2017). Auditory processing in noise is associated with complex

patterns of disrupted functional connectivity in autism spectrum disorder. Autism Research, 10(4), 631–647. 10.1002/aur.1714 [PubMed: 27910247]

Mamashli F, Khan S, Bharadwaj H, Losh A, Pawlyszyn SM, Hämäläinen MS, & Kenet T (2018). Maturational trajectories of local and long-range functional connectivity in autism during face processing. Human Brain Mapping, 39(10), 4094–4104. 10.1002/hbm.24234 [PubMed: 29947148]

Mamashli F, Hämäläinen M, Ahveninen J, Kenet T, & Khan S (2019). Permutation statistics for connectivity analysis between regions of interest in EEG and MEG data. Scientific Reports, 9(1), 1–10. 10.1038/s41598-019-44403-z [PubMed: 30626917]

Mamashli F, Khan S, Obleser J, Friederici AD, & Maess B (2019). Oscillatory dynamics of cortical functional connections in semantic prediction. Human Brain Mapping, 40(6), 1856–1866. 10.1002/hbm.24495 [PubMed: 30537025]

Maris E, & Oostenveld R (2007). Nonparametric statistical testing of EEG- and MEG-data. Journal of Neuroscience Methods, 164(1), 177–190. [PubMed: 17517438]

Mayer JS, Bittner RA, Nikolić D, Bledowski C, Goebel R, & Linden DEJ (2007). Common neural substrates for visual working memory and attention. NeuroImage, 36(2), 441–453. 10.1016/j.neuroimage.2007.03.007 [PubMed: 17462914]

McIntosh AR, & Lobaugh NJ (2004). Partial least squares analysis of neuroimaging data: Applications and advances. NeuroImage, 23 (suppl. 1), 250–263. 10.1016/j.neuroimage.2004.07.020

McPartland J, Dawson G, Webb SJ, Panagiotides H, & Carver LJ (2004). Event-related brain potentials reveal anomalies in temporal processing of faces in autism spectrum disorder. Journal of Child Psychology and Psychiatry and Allied Disciplines, 45(7), 1235–1245. 10.1111/j.1469-7610.2004.00318.x

Michaels TI, Long LL, Stevenson IH, Chrobak JJ, & Chen C-MA (2018). Effects of chronic ketamine on hippocampal cross-frequency coupling: Implications for schizophrenia pathophysiology. European Journal of Neuroscience, 48(8), 2903–2914. 10.1111/ejn.13822

Nakai T, Nagai T, Wang R, Yamada S, Kuroda K, Kaibuchi K, & Yamada K (2014). Alterations of GABAergic and dopaminergic systems in mutant mice with disruption of exons 2 and 3 of the Disc1 gene. Neurochemistry International, 74, 74–83. 10.1016/j.neuint.2014.06.009 [PubMed: 24973713]

Neumann D, Spezio ML, Piven J, & Adolphs R (2006). Looking you in the mouth: Abnormal gaze in autism resulting from impaired top-down modulation of visual attention. Social Cognitive and Affective Neuroscience, 1, 194–202. 10.1093/scan/nsl030 [PubMed: 18985106]

O'Neil EB, Hutchison RM, McLean DA, & Köhler S (2014). Resting-state fMRI reveals functional connectivity between face-selective perirhinal cortex and the fusiform face area related to face inversion. NeuroImage, 92, 349–355. 10.1016/j.neuroimage.2014.02.005 [PubMed: 24531049]

Papathomas TV, & Bono LM (2004). Experiments with a hollow mask and a reverspective: Top-down influences in the inversion effect for 3-D stimuli. Perception, 33(9), 1129–1138. 10.1068/p5086 [PubMed: 15560511]

Pedregosa F, Varoquaux G, Gramfort A, Michel V, Thirion B, Grisel O, Blondel M, Prettenhofer P, Weiss R, Dubourg V, Vanderplas J, Passos A, Cournapeau D, Brucher M, Perrot M, & Duchesnay E (2011). Scikit-learn: Machine learning in python. Journal of Machine Learning Research, 12, 2825–2830.Retrieved from. http://scikit-learn.sourceforge.net

Pelli DG (1997). The VideoToolbox software for visual psychophysics: Transforming numbers into movies. Spatial Vision, 10(4), 437–442.Retrieved from. https://brill.com/view/journals/sv/10/4/article-p437_16.xml [PubMed: 9176953]

Port RG, Berman JI, Liu S, Featherstone RE, Roberts TPL, & Siegel SJ (2019). Parvalbumin cell ablation of NMDA-R1 leads to altered phase, but not amplitude, of gamma-band cross-frequency coupling. Brain Connectivity, 9(3), 263–272. 10.1089/brain.2018.0639 [PubMed: 30588822]

Port RG, Dipiero MA, Ku M, Liu S, Blaskey L, Kuschner ES, Edgar JC, Roberts TPL, & Berman JI (2019). Children with autism Spectrum disorder demonstrate regionally specific altered resting-state phase-amplitude coupling. Brain Connectivity, 9(5), 425–436. 10.1089/brain.2018.0653 [PubMed: 30900464]

Rossion B, Gauthier I, Tarr MJ, Despland P, Bruyer R, Linotte S, & Crommelinck M (2000). The N170 occipitotemporal component is delayed and enhanced to inverted faces but not to inverted

objects: An electrophysiological account of face-specific processes in the human brain. Neuroreport, 11(1), 69–74. 10.1097/00001756-200001170-00014 [PubMed: 10683832]

Rubia K (2013). Functional brain imaging across development. European Child and Adolescent Psychiatry, 22(12), 719–731. 10.1007/s00787-012-0291-8 [PubMed: 22729957]

Rutter M, Bailey A, & Lord C (2003). The social communication questionnaire: Manual. Los Angeles, CA: Western Psychological Services.

Seymour RA, Rippon G, Gooding-Williams G, Schoffelen JM, & Kessler K (2019). Dysregulated oscillatory connectivity in the visual system in autism spectrum disorder. Brain, 142, 3294–3305. 10.1093/brain/awz214 [PubMed: 31410480]

Sinha P, Kjelgaard MM, Gandhi TK, Tsourides K, Cardinaux AL, Pantazis D, Diamond SP, & Held RM (2014). Autism as a disorder of prediction. Proceedings of the National Academy of Sciences of the United States of America, 111 (42), 15220–15225. 10.1073/pnas.1416797111 [PubMed: 25288765]

Tang J, Falkmer M, Horlin C, Tan T, Vaz S, & Falkmer T (2015). Face recognition and visual search strategies in autism spectrum disorders: Amending and extending a recent review by Weigelt et al. PLoS One, 10(8), e0134439. 10.1371/journal.pone.0134439 [PubMed: 26252877]

Taulu S, & Simola J (2006). Spatiotemporal signal space separation method for rejecting nearby interference in MEG measurements. Physics in Medicine and Biology, 51(7), 1759–1768. 10.1088/0031-9155/51/7/008 [PubMed: 16552102]

Taulu S, Kajola M, & Simola J (2004). Suppression of interference and artifacts by the signal space separation method. Brain Topography, 16(4), 269–275. 10.1023/B:BRAT.0000032864.93890.f9 [PubMed: 15379226]

Tavares PP, Mouga SS, Oliveira GG, & Castelo-Branco M (2016). Preserved face inversion effects in adults with autism spectrum disorder. Neuroreport, 27(8), 587–592. 10.1097/WNR.0000000000000576 [PubMed: 27092469]

Teunisse JP, & de Gelder B (2003). Face processing in adolescents with autistic disorder: The inversion and composite effects. Brain and Cognition, 52(3), 285–294. 10.1016/S0278-2626(03)00042-3 [PubMed: 12907173]

Tottenham N, Tanaka JW, Leon AC, McCarry T, Nurse M, Hare TA, Marcus DJ, Westerlund A, Casey BJ, & Nelson C (2009). The NimStim set of facial expressions: Judgments from untrained research participants. Psychiatry Research, 168(3), 242–249. 10.1016/j.psychres.2008.05.006 [PubMed: 19564050]

Uutela K, Taulu S, & Hämäläinen M (2001). Detecting and correcting for head movements in neuromagnetic measurements. NeuroImage, 14(6), 1424–1431. 10.1006/nimg.2001.0915 [PubMed: 11707098]

Vakorin VA, Doesburg SM, Leung RC, Vogan VM, Anagnostou E, & Taylor MJ (2017). Developmental changes in neuromagnetic rhythms and network synchrony in autism. Annals of Neurology, 81, 199–211. 10.1002/ana.24836 [PubMed: 27977875]

Webb SJ, Merkle K, Murias M, Richards T, Aylward E, & Dawson G (2012). ERP responses differentiate inverted but not upright face processing in adults with ASD. Social Cognitive and Affective Neuroscience, 7(5), 578–587. 10.1093/scan/nsp002 [PubMed: 19454620]

Weigelt S, Koldewyn K, & Kanwisher N (2012). Face identity recognition in autism spectrum disorders: A review of behavioral studies. Neuroscience & Biobehavioral Reviews, 36(3), 1060–1084. 10.1016/j.neubiorev.2011.12.008 [PubMed: 22212588]

Wright B, Alderson-Day B, Prendergast G, Bennett S, Jordan J, Whitton C, Gouws A, Jones N, Attur R, Tomlinson H, & Green G (2012). Gamma activation in young people with autism spectrum disorders and typically-developing controls when viewing emotions on faces. PLoS One, 7(7), e41326. 10.1371/journal.pone.0041326 [PubMed: 22859975]

Wulff P, Ponomarenko AA, Bartos M, Korotkova TM, Fuchs EC, Bähner F, Both M, Tort AB, Kopell NJ, Wisden W, & Monyer H (2009). Hippocampal theta rhythm and its coupling with gamma oscillations require fast inhibition onto parvalbumin-positive interneurons. Proceedings of the National Academy of Sciences of the United States of America, 106 (9), 3561–3566. 10.1073/pnas.0813176106 [PubMed: 19204281]

Yin RK (1969). Looking at upide-down faces. Journal of Experimental Psychology, 81(1), 141–145. 10.1037/h0027474

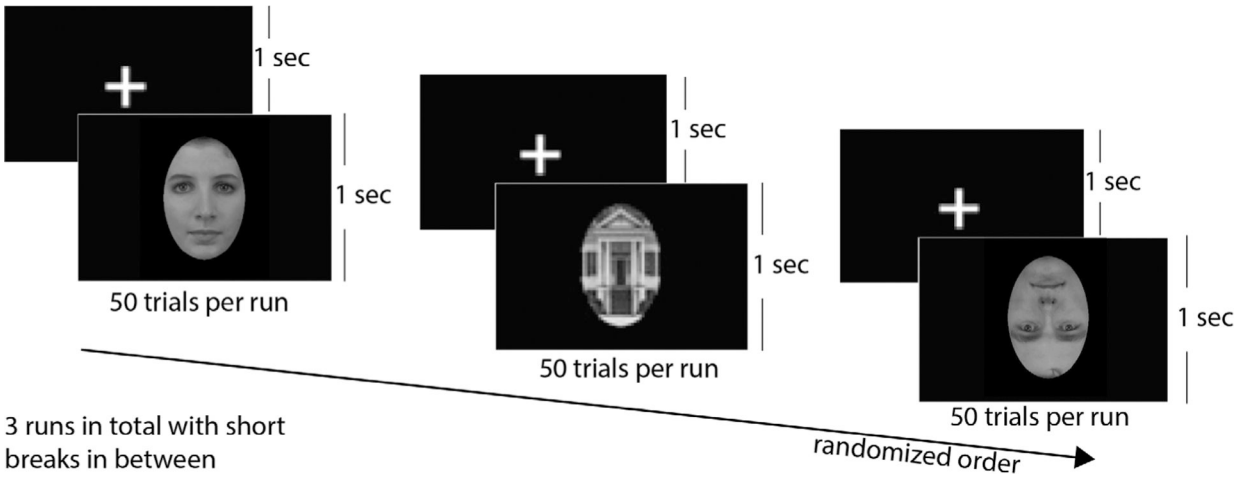

FIGURE 1.

A schematic representation of the stimulus. Each stimulus type was presented a minimum of 150 times, across three runs (~50 times per run per stimulus), in random order, for 1 s, with 1 s interstimulus interval consisting of a fixation cross. Two other stimulus categories not shown (or analyzed for this study) consisted of angry faces and fearful faces

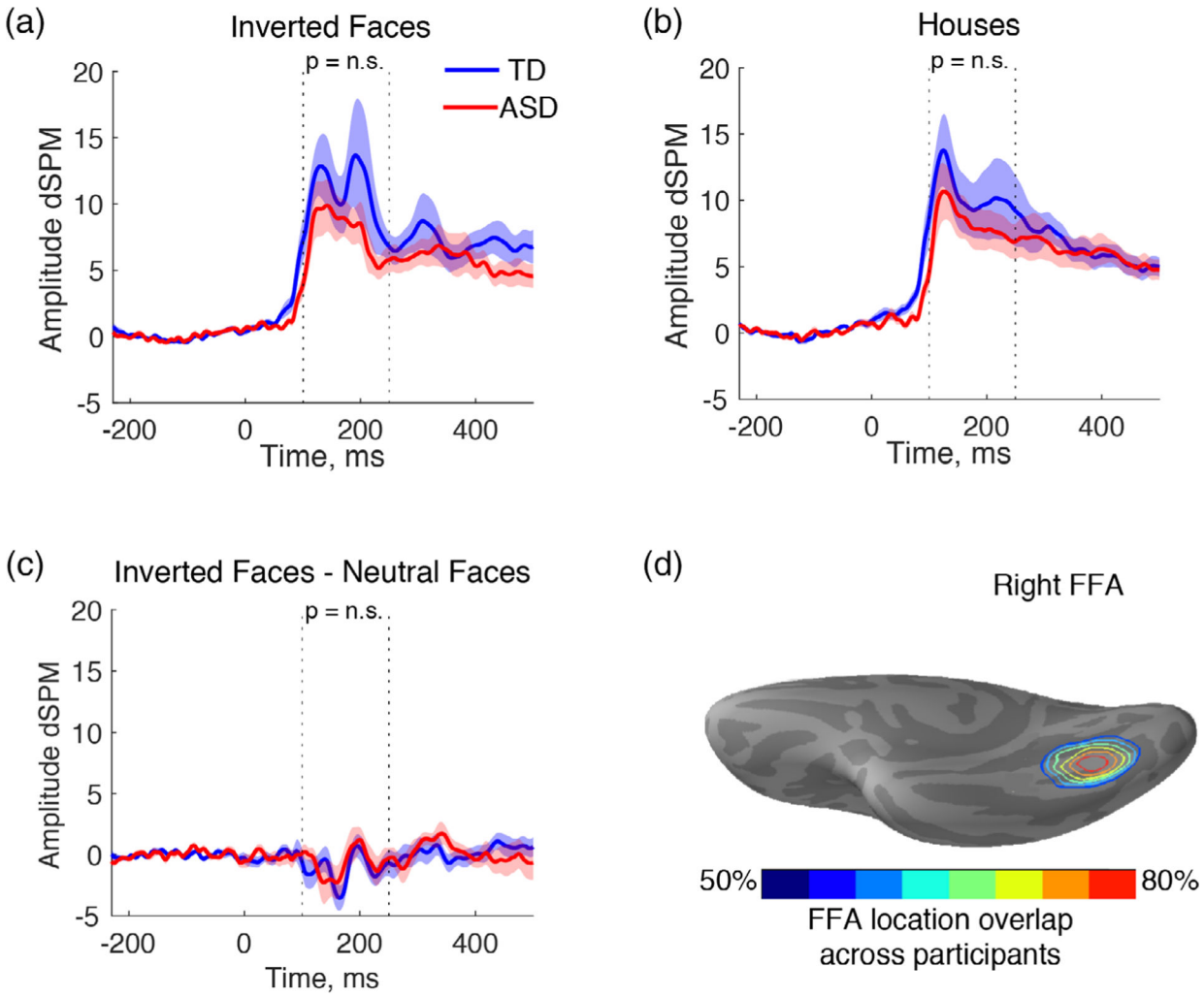

FIGURE 2.

Evoked responses. (a) Group average of evoked responses from the inverted faces condition. (b) Group average of evoked responses from the houses condition. (c) No differences in evoked responses to inverted neutral faces versus upright neutral faces. (d) Averaged FFA boundaries. Shaded area in a, b, c denotes the standard error

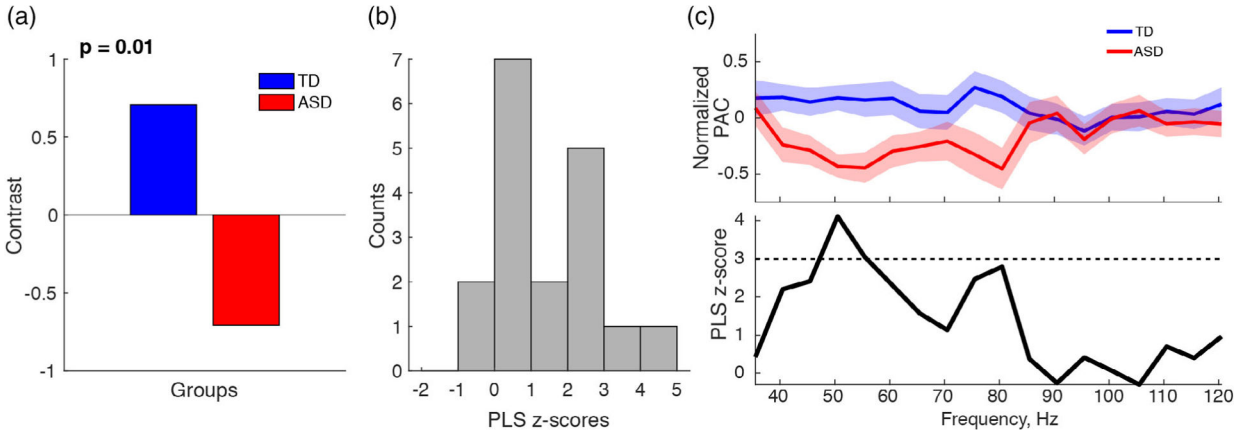

FIGURE 3.

Group Differences in PAC. (a) Group contrast computed using PLS. (b) Distribution of PLS *z*-score across frequencies. (c) Normalized PAC in FFA averaged across participants (upper panel) and *z*-score as a function of frequency with threshold of 3 to illustrate the most robust group differences (lower panel)

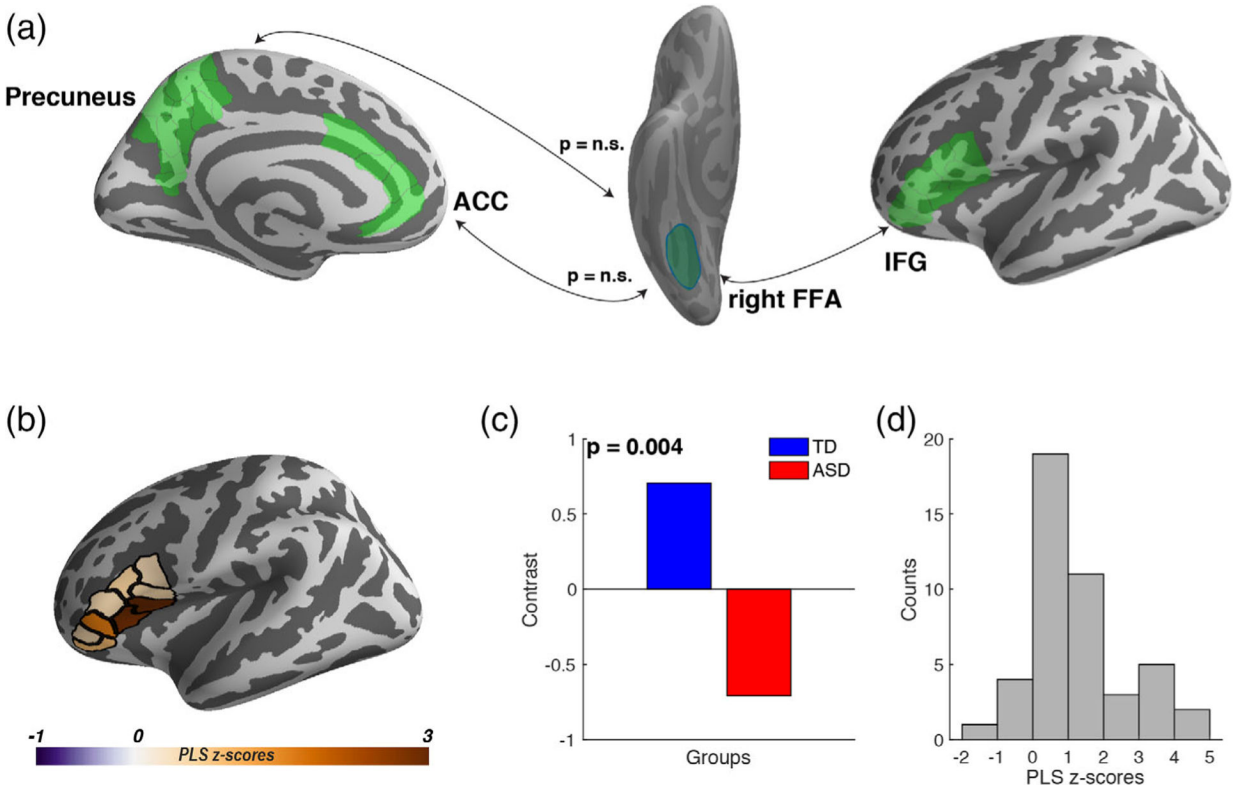

FIGURE 4.

Functional connectivity (*Z*-coherence) between the FFA and the IFG. (a) The ROIs that were used to compute coherence in the alpha band between the left IFG and the right FFA. (b) Brain surface with the *z*-score for coherence averaged across 8–13 Hz for sub-ROIs of the IFG, illustrating the sub-ROIs that contributed the most to the group difference in *Z*-coherence. (c) PLS contrast demonstrating group differences in *Z*-coherence between the right FFA and sub-ROIs of the left IFG. (d) PLS *z*-scores distribution associated with a group contrast

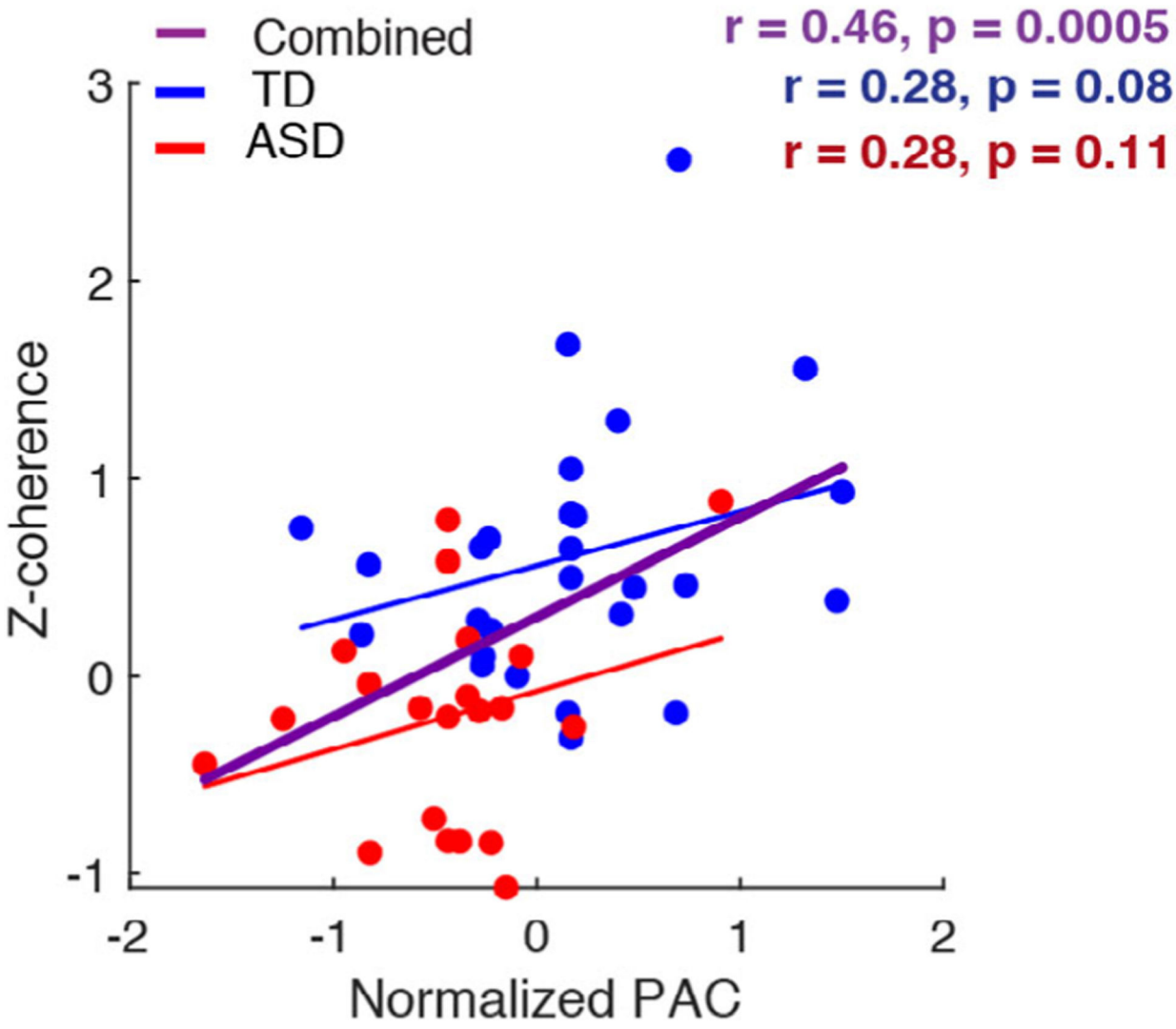

FIGURE 5.

Correlation between normalized PAC and IFG-FFA *Z*-coherence. Correlations between the magnitude of normalized PAC and of *Z*-coherence scores for the ASD group (red) and the TD group (blue), each separately, as well as the correlation when both groups were combined (purple). The correlation trended towards significance for each group separately, and was significant when both groups were combined

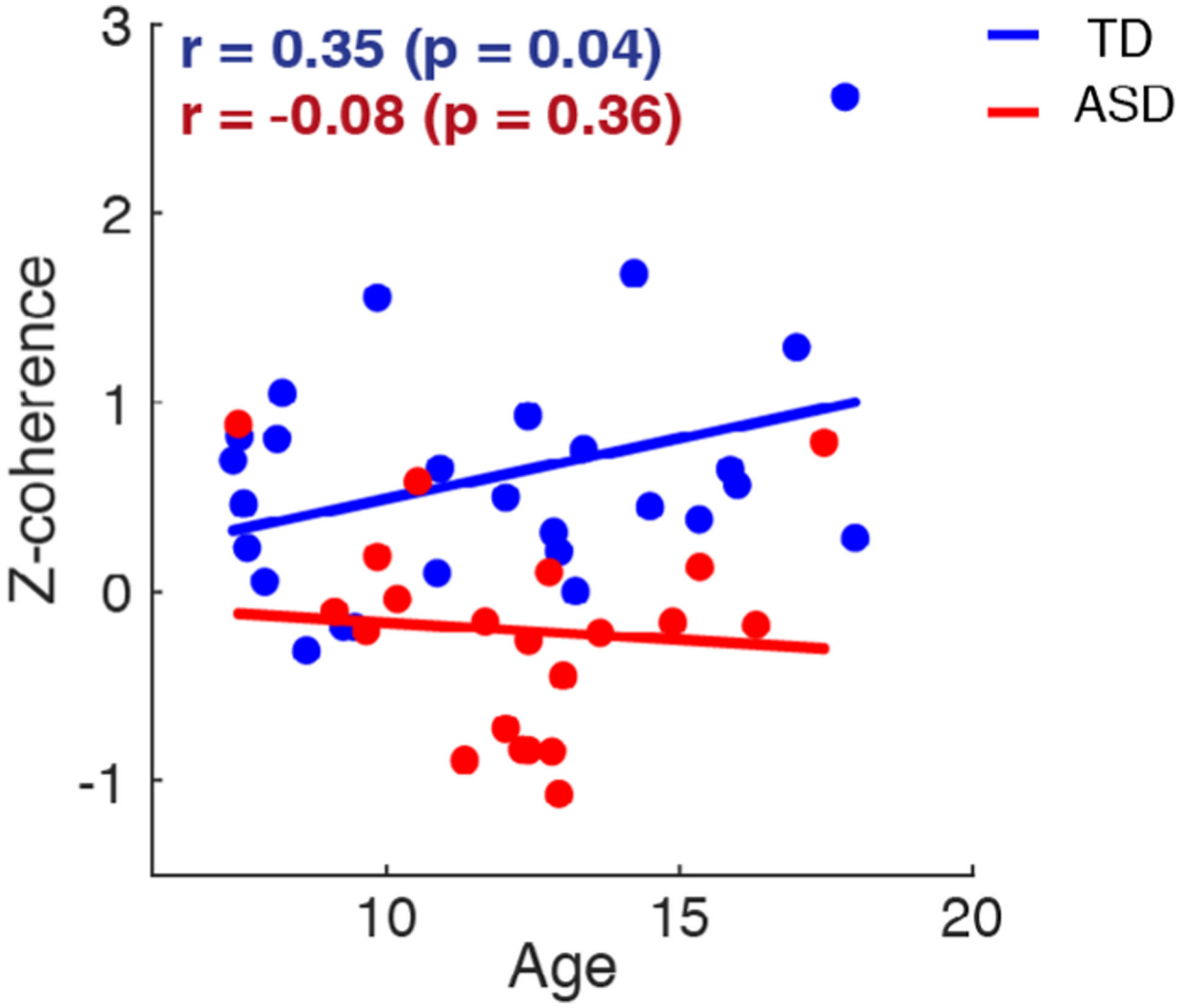

FIGURE 6.

Correlations between age and IFG-FFA *Z*-coherence. The correlation between age and IFG-FFA *Z*-coherence was significant for the TD group (blue), and not significant in the ASD group (red)

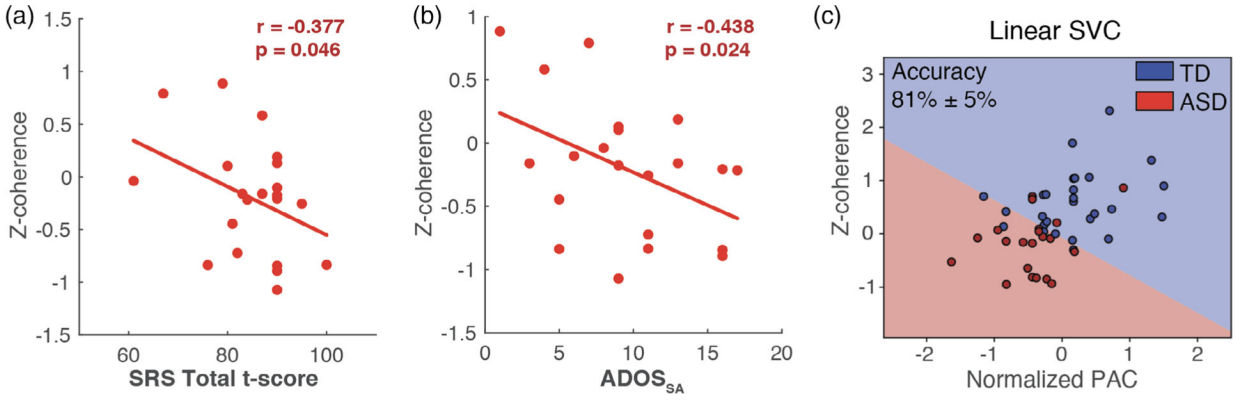

FIGURE 7.

Correlations between ASD phenotype and IFG-FFA *Z*-coherence, and group classification. (a) Correlation between IFG-FFA *Z*-coherence and SRS Total *t*-score in the ASD group. (b) Correlation between IFG-FFA *Z*-coherence and $ADOS_{SA}$ score in the ASD group. (c) A linear classifier using the PAC and *Z*-coherence values from the inverted faces condition had an accuracy of 81% in classifying participants by diagnosis

TABLE 1

Demographic information and behavioral score of the participants

	ASD	TD
Sample size (females)	21(2)	27 (4)
Age, years	12.3 ± 2.42	11.8 ± 3.45
Nonverbal IQ	109.0 ± 19.23	106.9 ± 11.42
Verbal IQ	108.2 ± 15.88	110.4 ± 15.03
SRS total *t*-score	84.9 ± 8.96	
ADOS social-affective (SA) sub-score	9.5 ± 4.59	